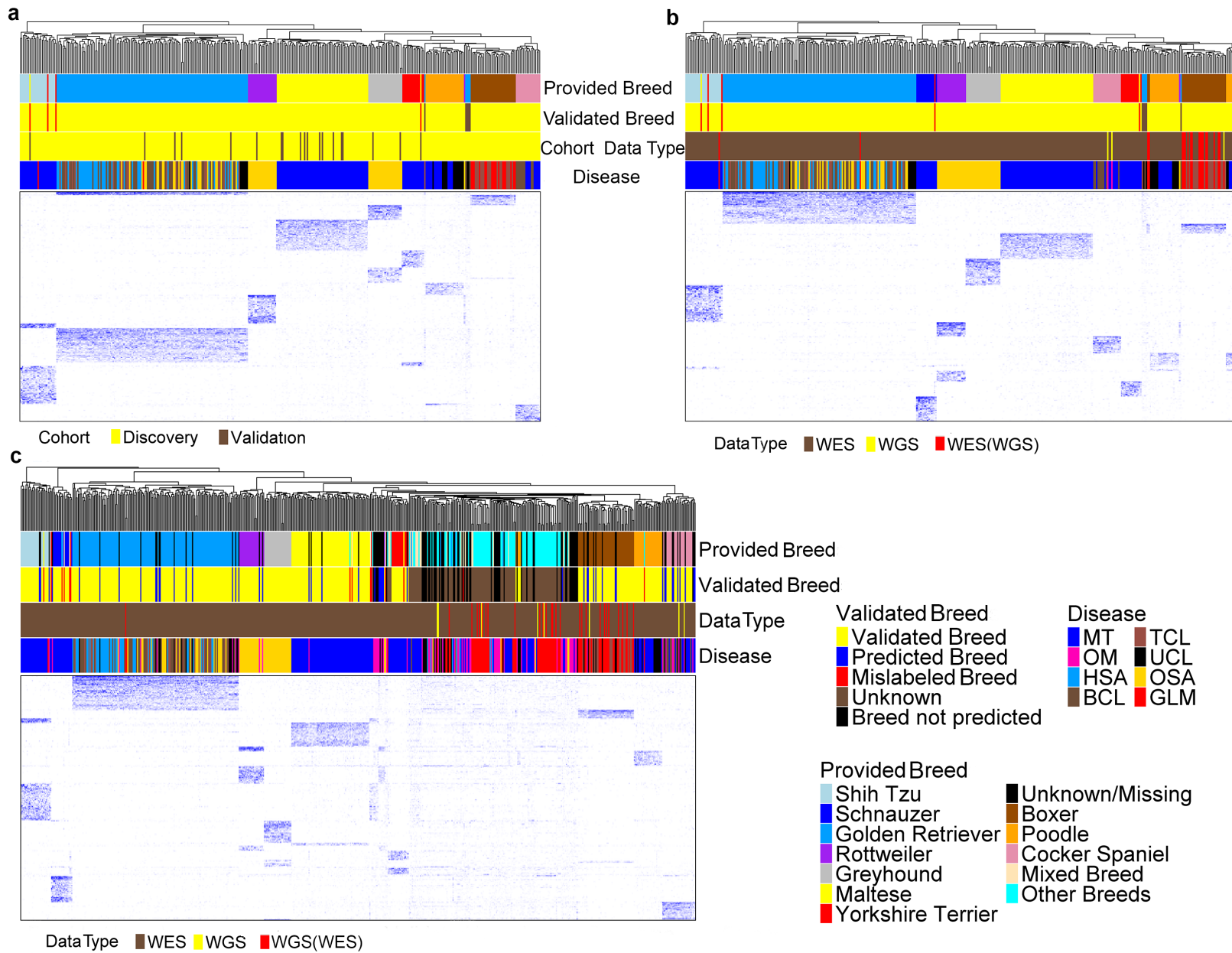


**Supplementary Figure 1. Whole-genome sequencing (WGS) data QC.** Among 172 paired tumor and normal samples from 86 dogs with published WGS data, a total of 72 samples from 36 dogs passed our QC (Supplementary Data 1). Panels **a-g** are presented as described in panels **a-c**

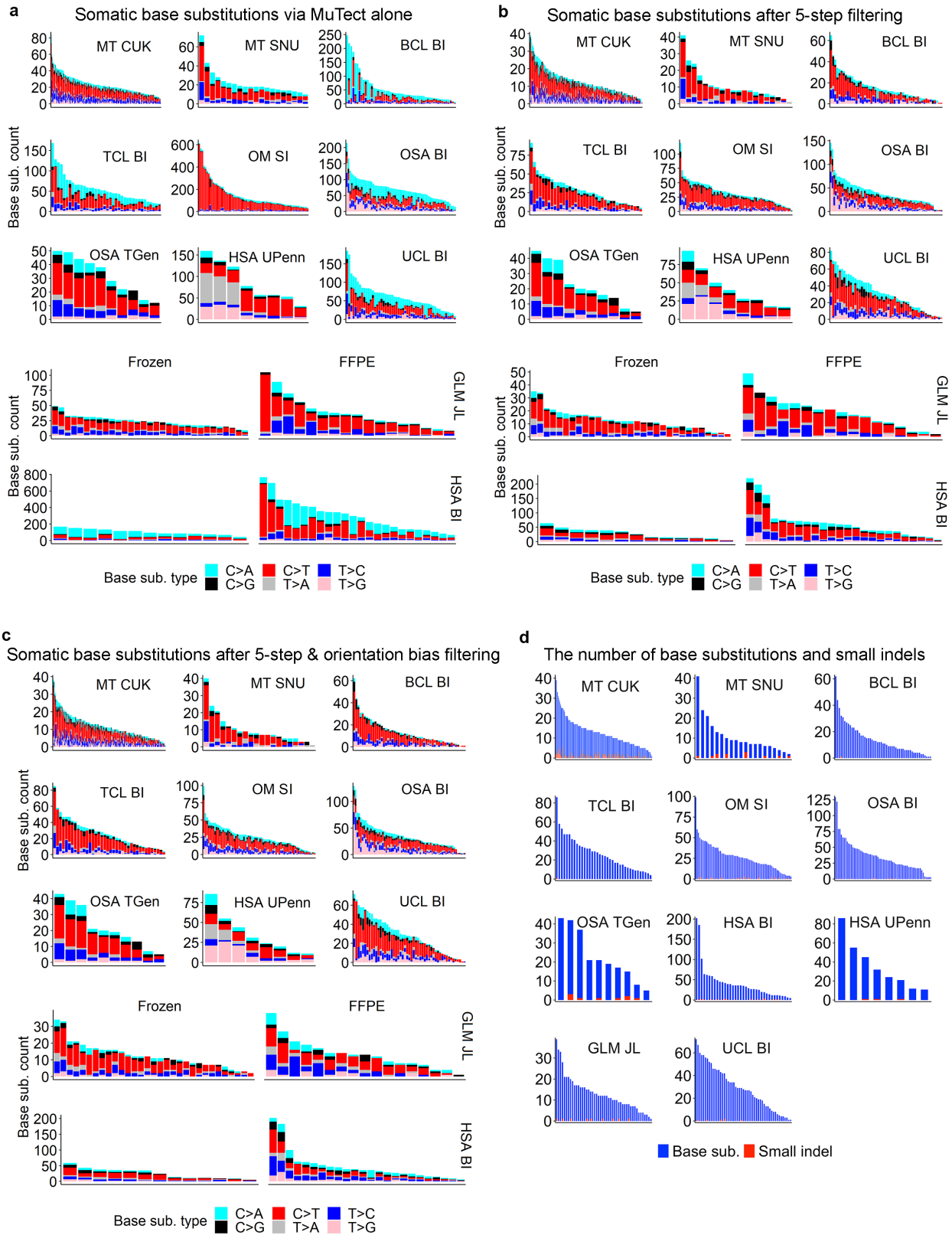
and **e-h** of Figure 1, respectively. **a-b**)  $n = 67$ , 4 and 15; **c-d**)  $n = 42$ , 4 and 15; and **e**)  $n = 36$  (33 normal), 4 (3 tumors) and 15 (0 normal samples) independent cases for matched normal and tumor samples of GLM, OM, and OSA respectively. **f-g**)  $n = 33$  and 3 independent cases of GLM and OM, respectively. Source data are provided as a Source Data file.



**Supplementary Figure 2. Corroboration of our breed validation and prediction strategy.**

- a.** The WES dataset is divided into the discovery cohort, which consists of large sample size studies and has 362 dogs, and the validation cohort, which consists of small sample size studies and has 19 dogs (Supplementary Data 2). The discovery cohort has 9 breeds with each having  $\geq 10$  dogs, which were used to identify breed-specific germline base substitution and small indel variants (Supplementary Data 2). VAF values of the identified 9 breed-specific variants (5,892 total; see Supplementary Data 2) were then used to cluster the animals from both the discovery and validation cohorts. The image is presented as described in Figure 2.
- b.** Corroboration with the WGS dataset. Dogs from both WES and WGS datasets were clustered with VAF values of the 10 breed-specific variants (see Figure 2). In the “Data type” bar, the “WES(WGS)” label represents dogs that have both WES and WGS data but were clustered here solely based on their WES data.
- c.** Corroboration with all 626 dogs from both WES and WGS datasets using the 10 breed-specific variants. All dogs with data that have passed QC shown in Figure 1 and Supplementary Figure 1 were clustered here, including dogs from mixed breeds or breeds with  $< 10$  animals. The image is presented as described in Figure 2.

Source data are provided as a Source Data file.



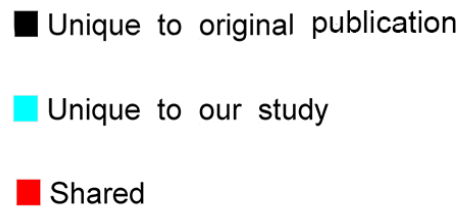
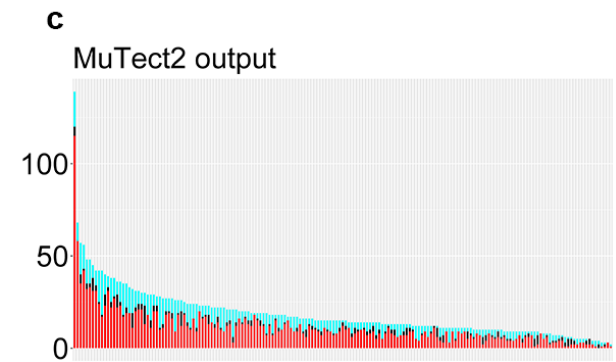
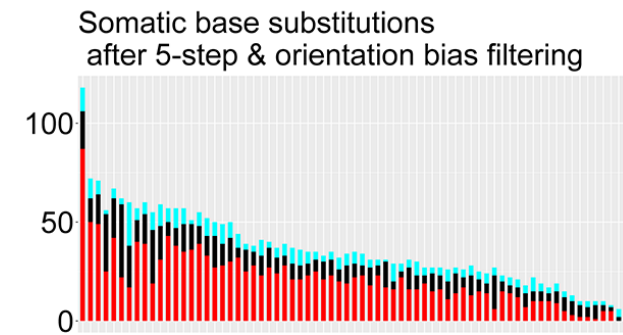
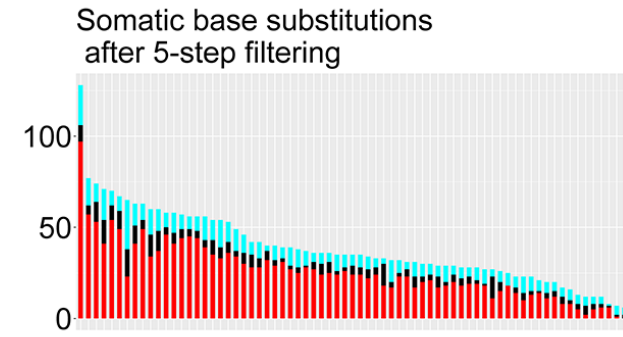
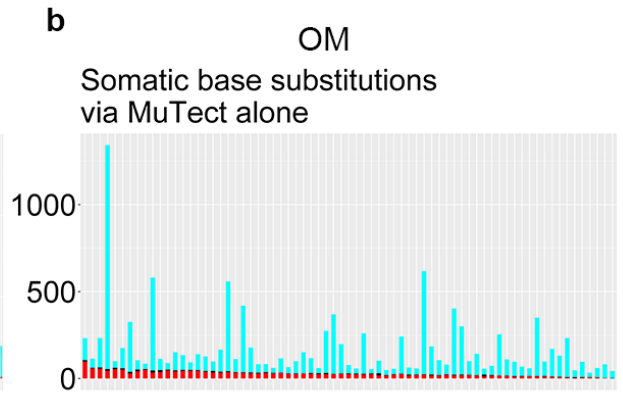
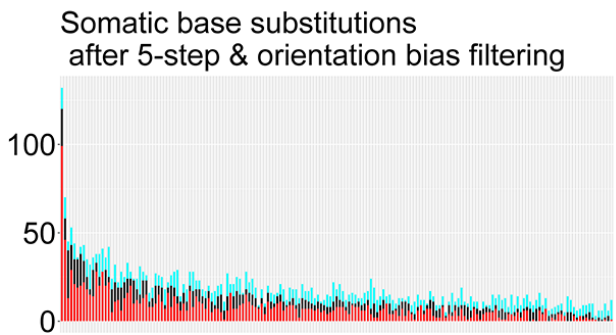
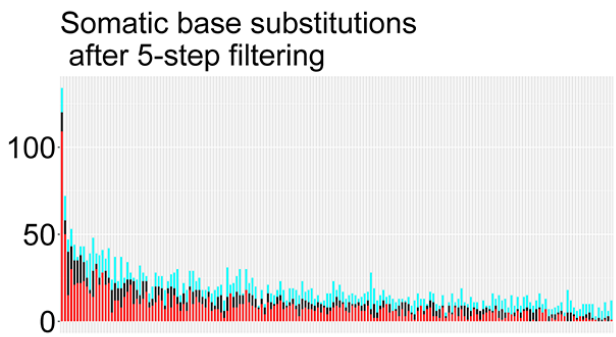
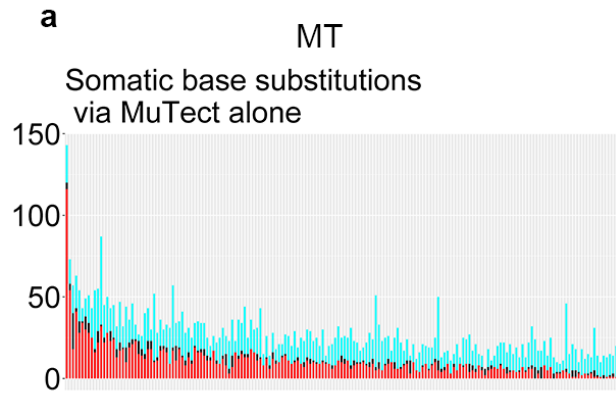
**Supplementary Figure 3. Somatic mutation discovery and filtering.**

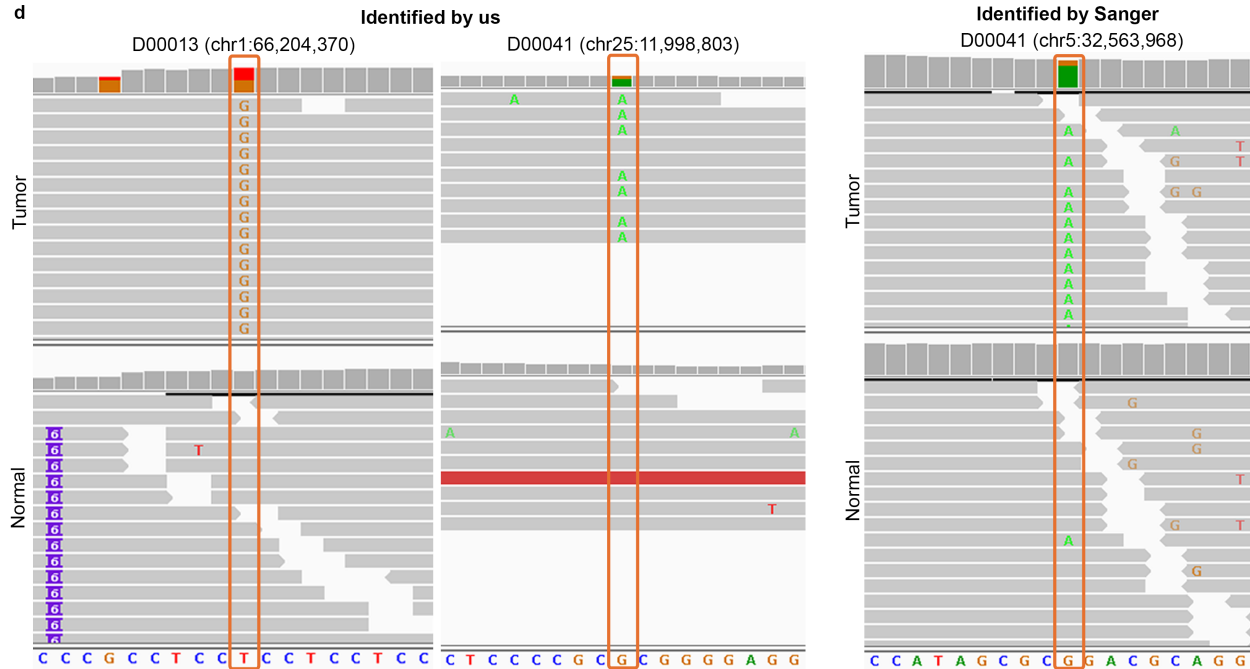
**a.** Distributions of the six base substitution counts in each tumor of each study called by MuTect. Each study is represented by the tumor type and the institute name. MT: mammary

tumor; GLM: glioma; BCL: B-cell lymphoma; TCL: T-cell lymphoma; OM: oral melanoma; OSA: osteosarcoma; HSA: hemangiosarcoma; UCL: unclassified. CUK: Catholic University of Korea; SNU: Seoul National University; JL: Jackson Laboratory; SI: Sanger Institute; BI: Broad Institute; UPenn: University of Pennsylvania.

- b.** Distributions of the six base substitution counts in each tumor of each study called by MuTect followed by 5-step filtering<sup>1</sup> (see Methods).
- c.** Distributions of the six base substitution counts in each tumor of each study called by MuTect, followed by the 5-step filtering<sup>1</sup> and paired-read strand orientation bias filtering (see Methods).
- d.** Distributions of base substitution and small indel counts in each tumor of each study. Base substitutions were discovered as described in **c**, and small indels were discovered with Strelka (see Methods). The results indicate very few small indels compared to base substitutions.

Source data are provided as a Source Data file.



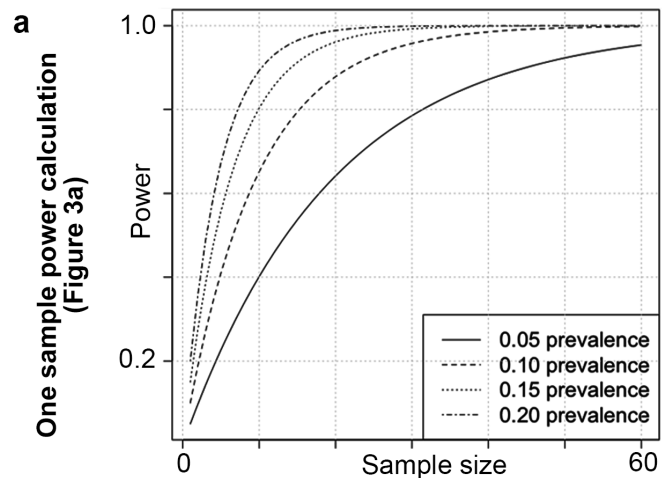


**Supplementary Figure 4. Comparison of somatic mutation findings between our study and the original publications.**

**a-c.** Mutations discovered at each of the three steps of our pipeline (see Supplementary Figure 3a-c) were compared to those from the original publications. For each mutation in each sample, the genomic coordinate and the actual mutation, which are published only for mammary tumor (MT)<sup>2</sup> (a) and oral melanoma (OM)<sup>1</sup> (b), were compared. Distributions of identical and different mutation counts in each sample were plotted. As the original MT publication<sup>2</sup> used MuTect2 instead of MuTect for mutation calling, we also conducted the analyses using MuTect2 and plotted the comparison (c).

**d.** Examples of somatic mutations found only by our study (left two images) or by the original publication (right image). Images are screen shots from the IGV program, with the tumor name provided (e.g., DD00013) and the mutation indicated by an orange rectangle. Source data are provided as a Source Data file.

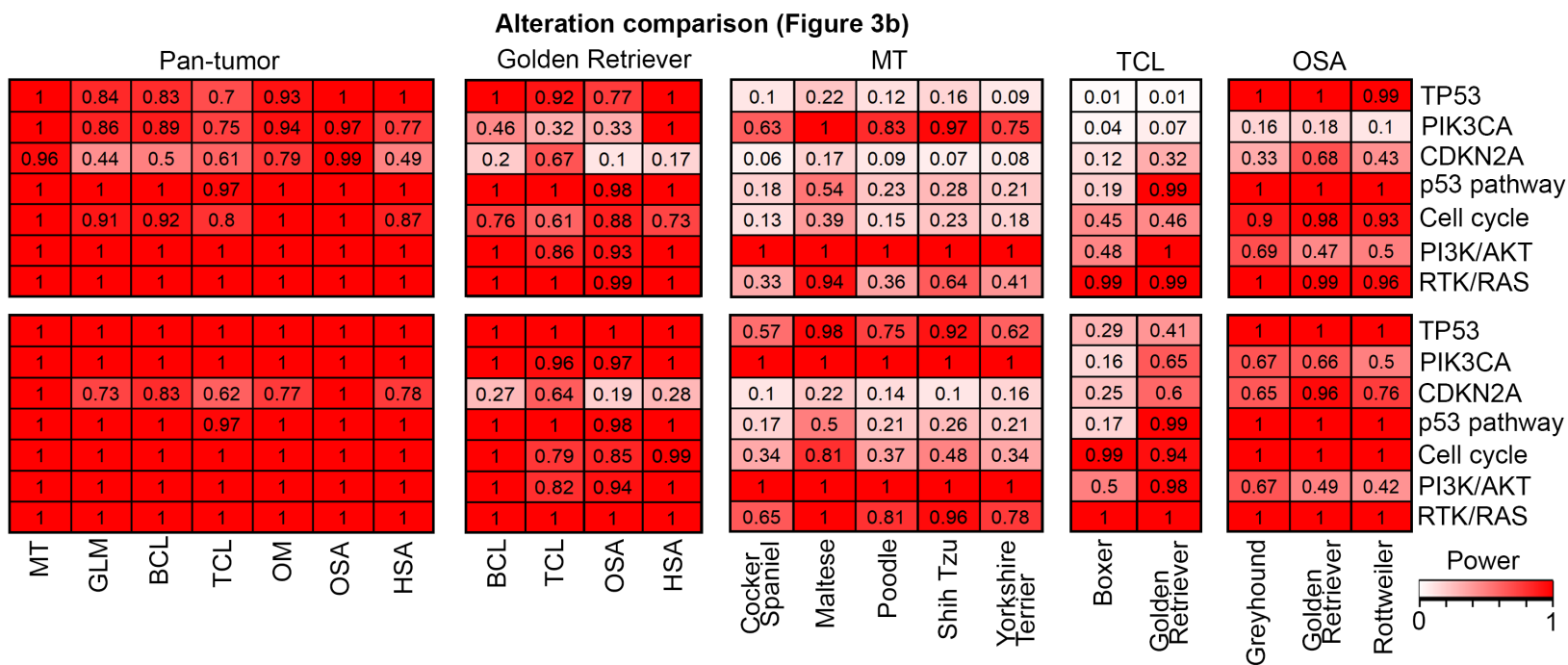




**b**

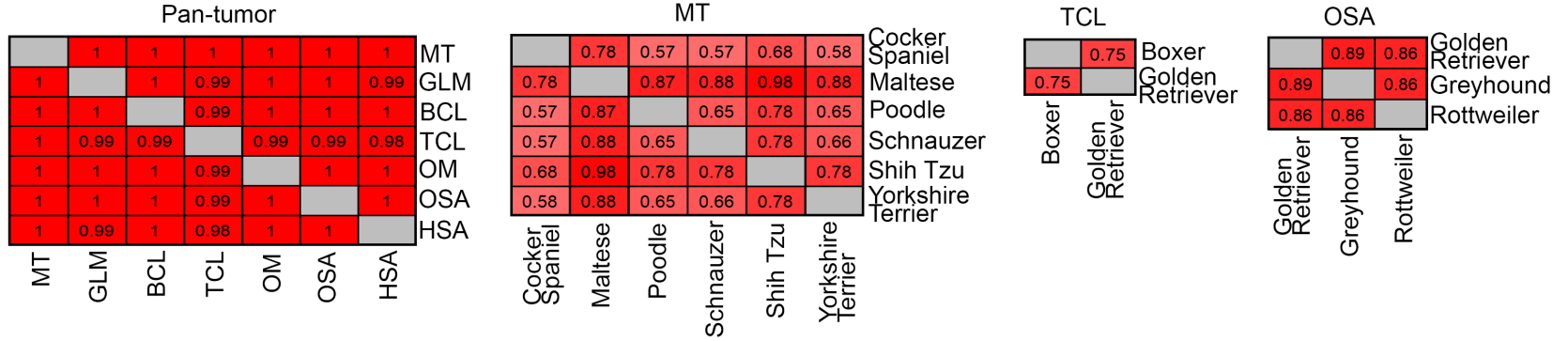
Presumed odds ratio varies by gene/pathway

Presumed odds ratio 2



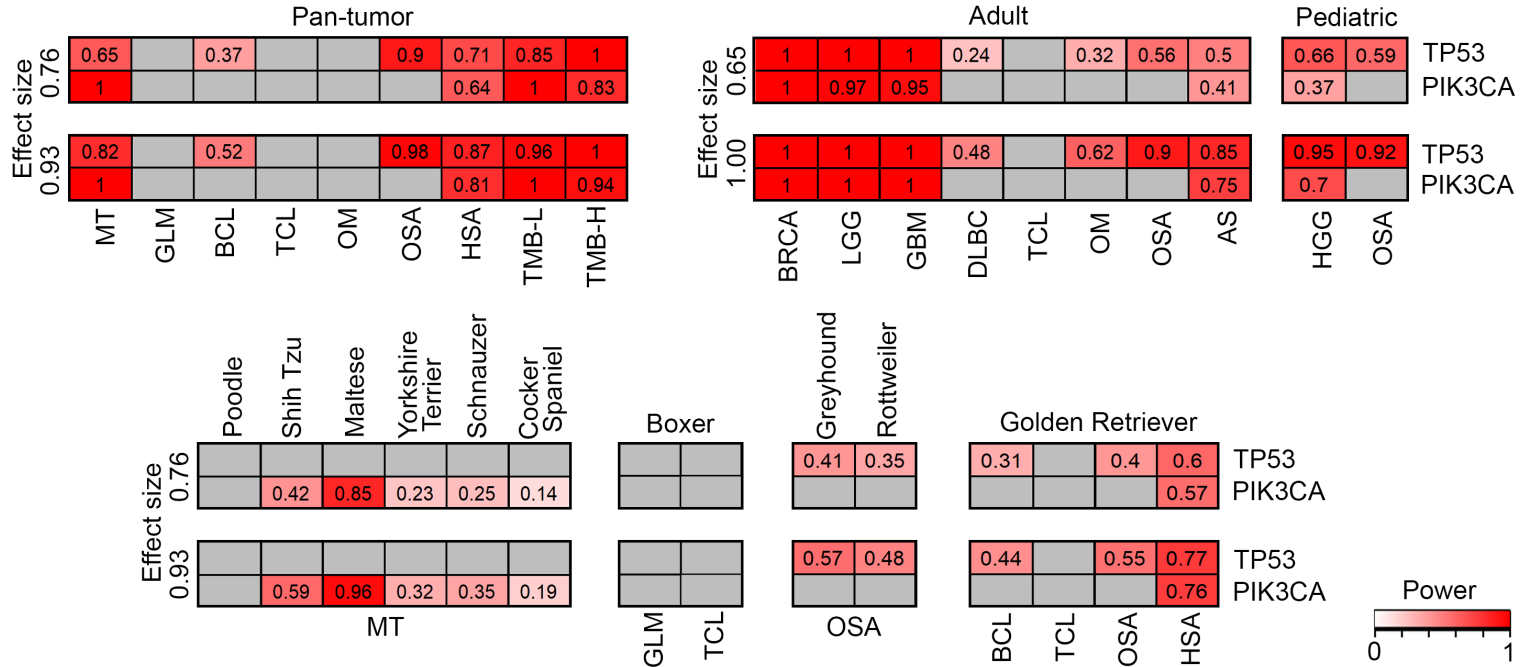
c

Cross-tumor / breed TMB differences (Figures 6a & 7a)



d

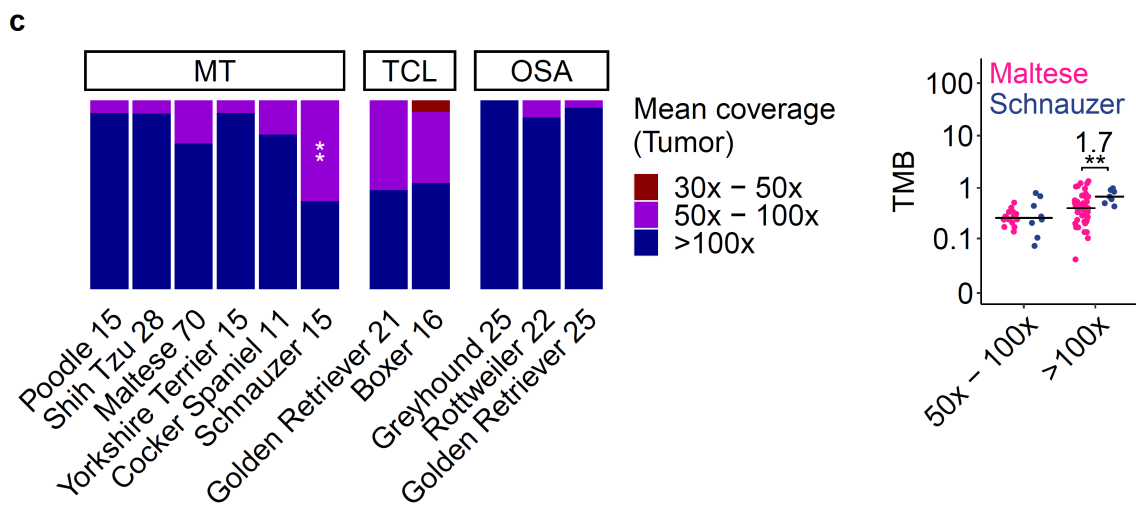
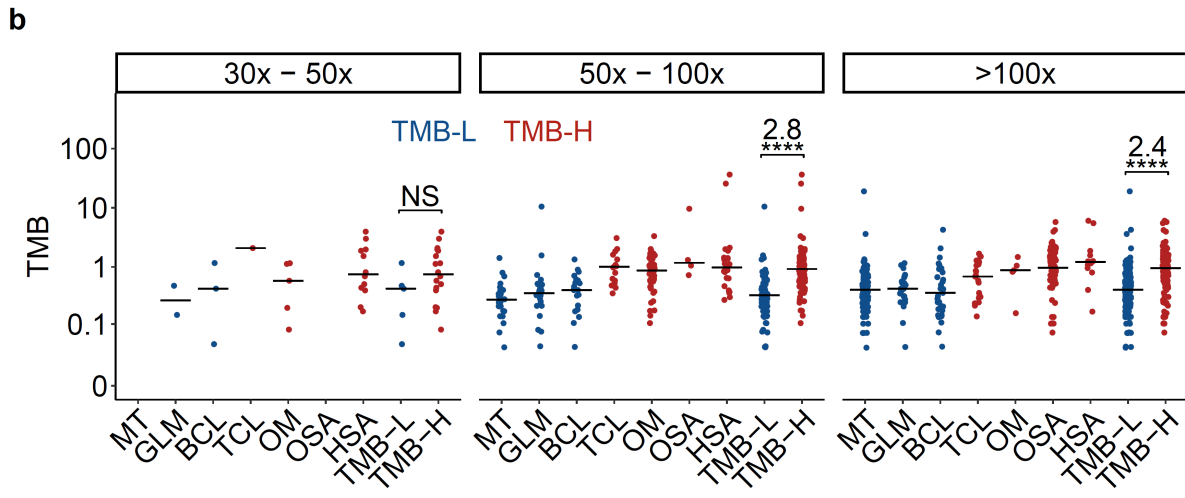
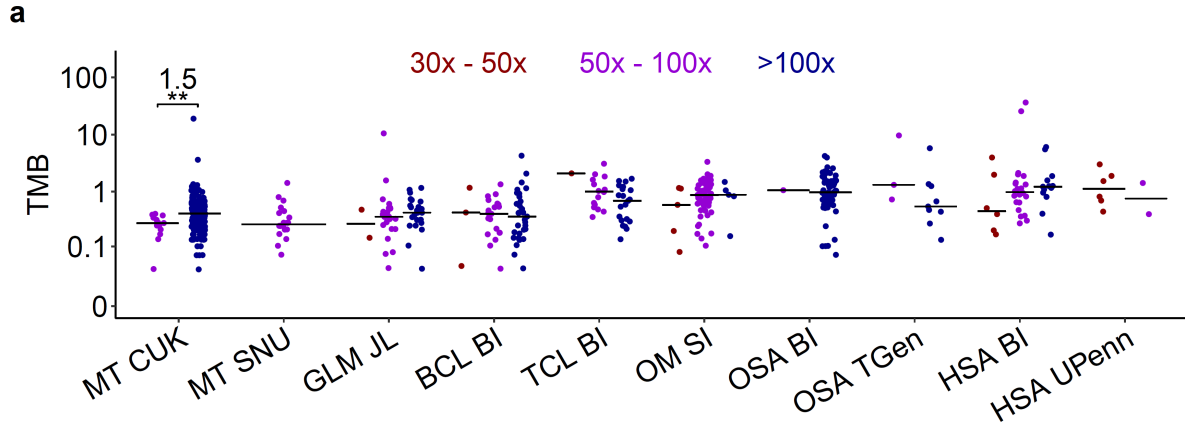
Mutation association with TMB (Figures 6b, 6c & 7b)



**Supplementary Figure 5. Power calculation.**

- a.** One-sample power calculation is for the mutation detection power. The power of detecting a mutation within a tumor type or breed is estimated based on the mutation prevalence and the sample size. Simulated curves were generated as described in Methods.
- b.** Two-sample Fisher exact test power. The power of each Fisher exact test shown in Figure 3b was calculated using: 1) the actual sample sizes of the two groups being compared; and 2) odds ratios as described in Methods.
- c.** Two-sample Wilcoxon test power for TMB comparison shown in Figures 6a and 7a. Each power was calculated using: 1) the actual sample sizes of the two groups being compared; and 2) an effect size as described in Methods.
- d.** Two-sample Wilcoxon test power for TMB-gene mutation association analysis shown in Figures 6b, 6c and 7b. The calculation is described in Methods.

Source data are provided as a Source Data file.

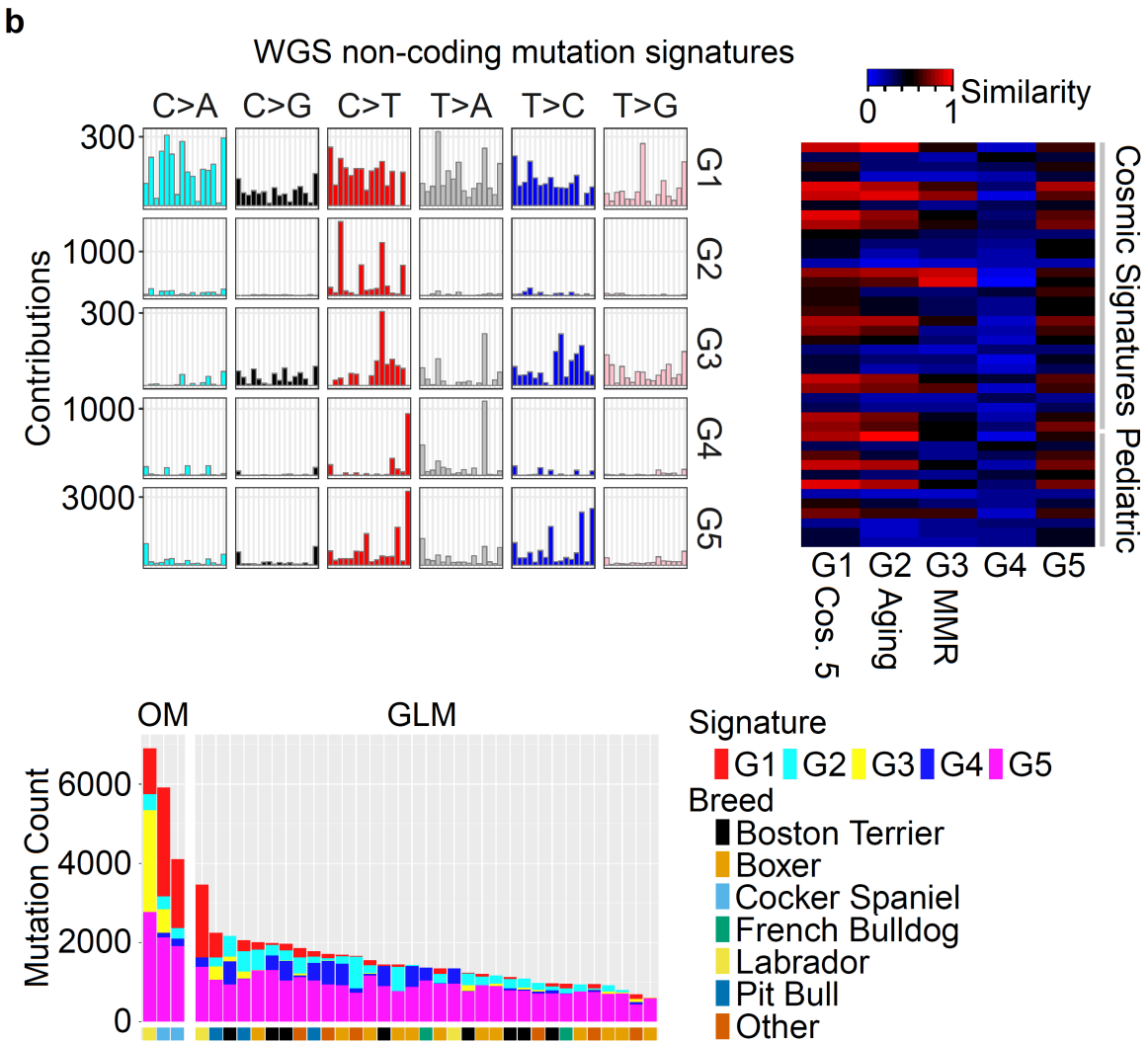
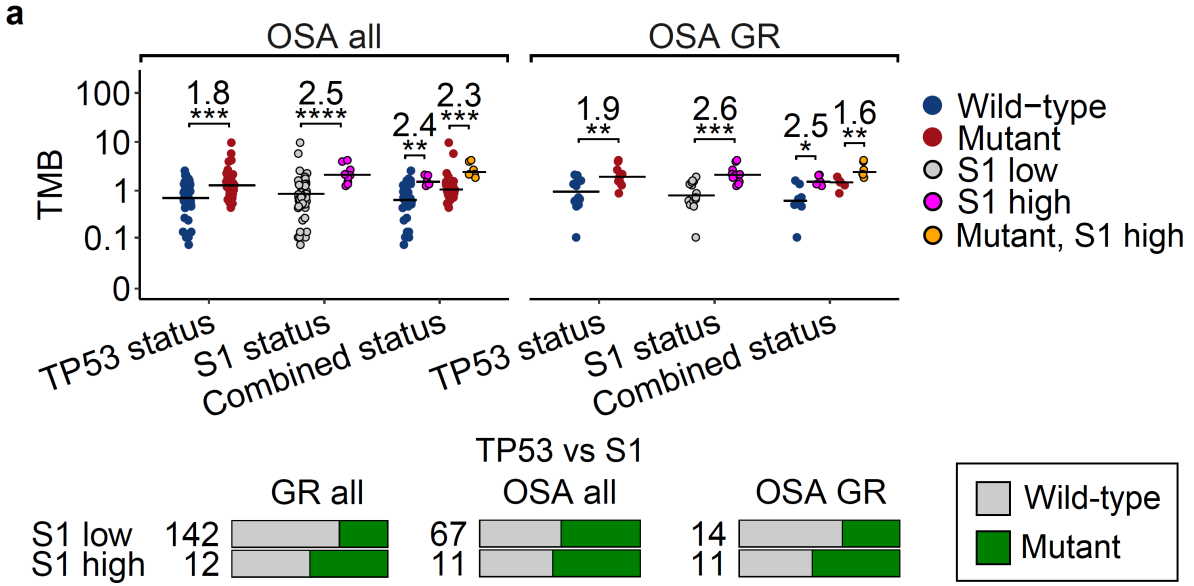


**Supplementary Figure 6. TMB at different sequence coverage of 30-50x, 50-100x and >100x.**

- a.** Distribution of tumor mean coverage in each WES study.  $n = 13, 169, 20, 2, 24, 23, 3, 21, 31, 1, 16, 21, 5, 61, 5, 1, 65, 3, 9, 6, 22, 13, 6$  and 2 independent tumors from left to right. Two-sided Wilcoxon tests were conducted as indicated; \*\*:  $p = 0.007$ .
- b.** TMB comparison at matched sequence coverage among tumor types.  $n = 0, 2, 3, 1, 5, 0, 12, 5, 18, 33, 24, 21, 16, 61, 4, 24, 78, 105, 169, 23, 31, 21, 5, 74, 13, 223$  and 113 independent tumors left to right. Two-sided Wilcoxon tests were conducted; NS (not significant):  $p = 0.1296$  and \*\*\*\*:  $p = 2.3678e-16$  (left) and  $7.3985e-18$  (right).
- c.** Distribution of tumor mean coverages among breeds within a study. The left plot indicates that only Schnauzer in MT has a coverage distribution differing from other breeds (\*\*:  $p = 0.002$  from two-sided Fisher exact test). The right plot shows that Schnauzer has a higher median TMB than Maltase at 100X coverage;  $n = 16, 8, 54$  and 7 independent tumors left to right; \*\*:  $p = 0.009$  from two-sided Wilcoxon tests. However, both plots indicate that the sample size of Schnauzer is small.

Source data are provided as a Source Data file.





**Supplementary Figure 8. S1 mutation signature is *TP53* mutation-independent, and noncoding mutation signature in WGS tumors.**

- a.** S1 mutation signature has a stronger association with TMB, compared to *TP53* mutation, within osteosarcoma in general (OSA all) and osteosarcoma Golden Retriever cases (OSA GR) (top). S1 is independent of *TP53* mutation (bottom).  $n = 39, 39, 67, 11, 34, 5, 33, 6, 14, 11, 14, 11, 9, 5, 5$  and 6 independent tumors from left to right. Two-sided Wilcoxon tests were conducted, with \*\*\*:  $p = 0.0009$ ; \*\*\*\*:  $p = 2.2e-5$ ; \*\*:  $p = 0.003$ ; \*\*\*:  $p = 0.0004$ ; \*\*:  $p = 0.003$ ; \*\*\*:  $p = 0.0003$ ; \*:  $p = 0.02$  and \*\*:  $p = 0.009$  from left to right.
- b.** Noncoding mutation signatures detected in 36 tumors with WGS data passing our QC measures. The top two plots are presented as described in Figure 8a, while the bottom plot indicates the mutation signature distribution in each tumor, with respective breeds indicated. Source data are provided as a Source Data file.

- 1 Wong, K. *et al.* Cross-species genomic landscape comparison of human mucosal melanoma with canine oral and equine melanoma. *Nat Commun* **10**, 353, doi:10.1038/s41467-018-08081-1 (2019).
- 2 Kim, T. M. *et al.* Cross-species oncogenic signatures of breast cancer in canine mammary tumors. *Nat Commun* **11**, 3616, doi:10.1038/s41467-020-17458-0 (2020).